Solubility of Dexamethasone in Supercritical Carbon Dioxide

ARTICLE *in* JOURNAL OF CHEMICAL & ENGINEERING DATA · DECEMBER 2012

Impact Factor: 2.04 · DOI: 10.1021/je301065f

5 AUTHORS, INCLUDING:

Rita Chim
University of Coimbra
2 PUBLICATIONS **10** CITATIONS
SEE PROFILE

Mara Elga Medeiros Braga
University of Coimbra
60 PUBLICATIONS **883** CITATIONS
SEE PROFILE

Ana M A Dias
University of Coimbra
60 PUBLICATIONS **870** CITATIONS
SEE PROFILE

Hermínio C De Sousa
University of Coimbra
95 PUBLICATIONS **1,740** CITATIONS
SEE PROFILE

Journal of chemical & engineering data

Article

pubs.acs.org/jced

Solubility of Dexamethasone in Supercritical Carbon Dioxide

R. B. Chim, M. B. C. de Matos, M. E. M. Braga, A. M. A. Dias,* and H. C. de Sousa*

CIEPQPF, Chemical Engineering Department, University of Coimbra, Rua Sílvio Lima, Pólo II-Pinhal de Marrocos, 3030-790 Coimbra, Portugal

ABSTRACT: Dexamethasone (DXMT) is a glucocorticoid that belongs to an important class of synthetic steroid hormones with potential to treat chronic immune and inflammatory diseases. In this work, the solid solubility of dexamethasone in supercritical carbon dioxide ($scCO_2$) was measured using a static method. Experimental data were measured at (308.2, 318.2, and 328.2) K in the pressure range from (15.1 to 35.7) MPa. The solubility in $scCO_2$ was found to be low and between ($1.25 \cdot 10^{-6}$ or $9.1 \cdot 10^{-3}$) kg·m^{-3} (at 308.2 K and 15.1 MPa) and ($2.81 \cdot 10^{-6}$ or $22.0 \cdot 10^{-3}$) kg·m^{-3} (at 328.2 K and 34.8 MPa) in terms of mole fraction or mass of drug per volume of solvent, respectively. Experimental data were correlated using semiempirical density based models (Méndez-Santiago−Teja, Bartle, and Chrastil). Obtained average absolute relative deviation [AARD (%)] values were lower than 13 %.

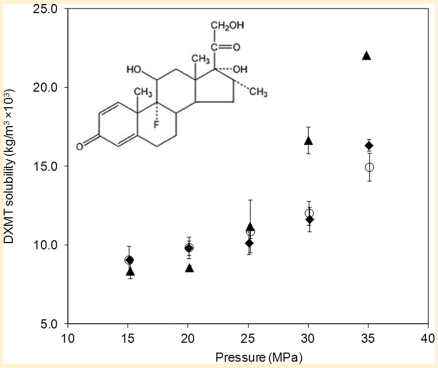

INTRODUCTION

Glucocorticoids (GCs) are the most important class of steroid hormones and are commonly used to treat chronic immune and inflammatory diseases that actuate as back regulators for the expression of anti- and pro-inflammatory proteins.[1−4] Dexamethasone (9-fluoro-11β,17,21-trihydroxy-16α-methylpregna-1,4-diene-3,20-dione) is a synthetic glucocorticoid that mimics the action of the most important GC of the human adrenal cortex, cortisol, which has an important role in immunologic, cardiovascular, homeostatic, and metabolic functions.[3−5] Due to its potent inflammatory actions and immunosuppressive properties, DXMT is used to regulate the production of several pro-inflammatory cytokines such as IL-1β, IL-6, INF-γ, and TNF-α.[6] It is also known to act as a potent modulator for the osteogenic differentiation of mesenchymal stem cells (as well as to stimulate osteoblastic maturation).[7−9]

Several studies reported the benefits of DXMT for bone tissue engineering applications.[10−14] However, and despite its already proved efficiency, the use of DXMT is still limited by the conventional administration methods since they are not target-specific and high doses may cause several side effects. A suitable alternative strategy would be its local sustained delivery by drug-loaded devices/scaffolds for intra-articular delivery.[6−8,15] Biomaterials such as polymers, polymer-based composites, bioglasses, calcium hydroxyapatite, calcium phosphate and silica bone cements, and polymeric/inorganic nanomaterials can be used as drug carriers for this drug, and they can be processed/tailored using $scCO_2$-based technologies. This will avoid the use of conventional organic solvents that may cause toxicity or processing methods that may promote chemical and thermal degradation.[16−23] These techniques are also frequently applied to promote drug particle size reduction by micronization.[24−26] The micronization of dexamethasone-21-acetate (using an aerosol solvent extraction system) was already employed to reduce drug particle sizes and to improve its dissolution properties and bioavailability.[27] Nanoparticles of PLGA were also used to microencapsulate dexamethasone phosphate using carbon dioxide as an antisolvent.[20] Chitosan and starch/PLA scaffolds were also processed and loaded with DXMT using supercritical carbon dioxide ($scCO_2$), originating materials with a loading yield of 0.14 mg drug/mg scaffold.[21,22] Despite the fact that this can be considered a relatively low DXMT loading yield, its activity is not compromised since it has been reported that the drug significantly enhanced the osteoclast-like cell formation after the pretreatment with 10^{-8} M DXMT.[7,28] Therefore, the use of $scCO_2$-based techniques to process polymers/composites, to solubilize/micronize drugs, and to impregnate/deposit drugs into adequate biomaterials for pharmaceutical/biomedical applications, are advantageous and "greener" alternatives to conventional techniques.[18,29]

In this work the equilibrium solubility of DXMT in $scCO_2$ was measured at different temperatures [(308.2, 318.2, and 328.2) K] in a pressure range between (15.1 and 35.7) MPa using a static analytic method coupled to a high-performance liquid chromatography (HPLC) quantification method. Experimental solubility data were correlated using semiempirical density-based models.

EXPERIMENTAL SECTION

Materials. The sources and purities of the materials used in this work are detailed in Table 1.

Experimental Solubility Measurement Procedures. Experimental equilibrium solubility data were measured according to the methodology previously reported in the literature.[30−34] In general terms, the solubility apparatus

Received: September 28, 2012
Accepted: November 16, 2012
Published: November 26, 2012

   dx.doi.org/10.1021/je301065f | J. Chem. Eng. Data 2012, 57, 3756−3760

Table 1. Purities and Source of the Solutes and Solvents That Were Used in This Work

chemical name	CAS	source	purity (w/w)
carbon dioxide	124-38-9	Praxair	0.9998
DXMT	50-02-2	Fluka	0.98
ethanol	200-578-6	Panreac Quimica SA	0.999
acetonitrile	75-05-B	Sigma-Aldrich	HPLC grade
methanol	67-56-1	Sigma-Aldrich	HPLC grade

comprises a high-pressure CO_2 syringe liquid pump and a sealed high pressure stainless steel vessel coupled to a known volume sampling loop, which is connected through a six-port sampling valve to sampling lines and to a balloon (used to quantify the amount of CO_2 for each data point), both with previously calibrated volumes. The high pressure cell is loaded with an excess amount of DXMT (≈ 200 mg) and a magnetic stirrer (700 rpm). After pressure and temperature stabilization, the mixture (CO_2 + drug) is stirred for 3 h followed by a stabilization period of 15 min. The temperature is maintained by means of thermostatic water baths to within ± 0.1 K, and pressure is measured by a high-pressure transducer (0 to 34.4) ± 0.04 MPa in the cell and (0 to 0.175) ± $1.9 \cdot 10^{-4}$ MPa in the calibrated balloon. After equilibrium, a portion (0.684 μL) of the saturated supercritical CO_2 is allowed to pass to the sampling loop. This volume was higher than the one used in previous works, to increase the solubilized sampling amount and decrease experimental error, due to the low solubility of the drug. Then the loop was depressurized into the collection vial, and ethanol is injected through the sample loop and the expansion lines to recover all of the sampled DXMT. The tubing lines are additionally cleaned/dried with fresh and slightly pressurized CO_2. The final volume of the solution was 5 mL. The amount of DXMT that was solubilized in $scCO_2$, at a given pressure and temperature conditions, was quantified by HPLC. The amount of CO_2 in each sampling step was calculated using the virial EOS (applied to pure CO_2). All of the prepared solutions were carefully stored and protected from light to avoid degradation. Each reported data point is the average of at least three replicate measurements.

High-Performance Liquid Chromatography (HPLC). Analyses were carried out using a HPLC system (Prominence UFLC Shimadzu coupled to a photo diode array detector SPD-M20A) and using a Eurospher column 100-5C18 RP (250 × 4 mm i.d., 5 mm, Germany) equipped with a precolumn. The chromatographic conditions were based on the ones previously reported in the literature.[35] A mobile phase, constituted by methanol/water in a proportion of 9:1 (v/v), was employed in an isocratic elution (15 min), at a flow rate of 1 $mL \cdot min^{-1}$ and at 35 °C. A run with acetonitrile only was used between each sample to clean the column. The chromatographic profile of each injected sample (20 μL) was measured at 239 nm in duplicate, and DXMT was identified and quantified by comparison of the retention times of standard solutions previously prepared in the concentration range between (0 and 120) $\mu g \cdot mL^{-1}$.

Correlation of Experimental Solubility Data Using Density-Based Correlations. Density-based semiempirical models were used to correlate the experimental equilibrium solubility data for DXMT in terms of reduced variables. The applied equations are given in Table 2, where T_r and P_r are the reduced experimental temperatures (T) and pressures (P), respectively, $S_{2,r}$ is the reduced solubility of the solid in the supercritical phase, $\rho_{r,1}$ is the solvent reduced density, and y_2 is the solute mole fraction. The critical properties of carbon dioxide where obtained from the NIST Chemistry Webbook.

Table 2. Summary of the Density-Based Models Used To Correlate the Experimental Solubility Data Measured for DXMT in $scCO_2$[a]

reduced variables (1 and 2 refer to $ScCO_2$ and DXMT, respectively)			
$S_{2,r} = (S_2/\rho_{c,1})$	$\rho_{1,r} = (\rho_1/\rho_{c,1})$	$T_r = (T/T_{c,1})$	$P_r = (P/P_{c,1})$
semiempirical density based models			
model	equation	adjusted constants	
Méndez-Santiago and Teja[36]	$T_r \ln (y_2 P_r) = A' + B'\rho_{r,1} + C'T_r$	$A' = -21.86$ $B' = 3.49$ $C' = 2.68$ AARD(%) = 13.1	
Bartle[37]	$\ln(y_2 P/P_{ref}) = a_1 + (a_2/T_r) + C(\rho_{r,1} - 1)$	$N = 15$ $a_1 = 0.67$ $a_2 = -14.95$ $C = 3.18$ AARD(%) = 13.4	
Chrastil[38]	$S_{2,r} = \rho_{r,1}^k \exp(\alpha + (\beta/T_r))$	$N = 15$ $k = 2.96$ $\alpha = -7.74$ $\beta = -4.94$ AARD(%) = 11.8	
		$N = 15$	

[a] P_{ref} is a standard pressure (set to 1 bar). The average absolute deviation (AARD) was calculated as: AARD (%) = $(100/N)\sum_{i=1}^{N}([y_{i,calc} - y_{i,exp}]/y_{i,exp})$ where N is the number of data points, $y_{i,exp}$ is the experimental solubility of the solid for experimental point i, and $y_{i,calc}$ is the calculated solubility for point i.

RESULTS AND DISCUSSION

Experimental data for the equilibrium solubility of DXMT in $scCO_2$ measured at (308.2, 318.2, and 328.2) K, and in the pressure range from (15 up to 35) MPa are presented in Table

Table 3. Experimental Solubility Data of DXMT in Supercritical Carbon Dioxide ($scCO_2$)[a]

T/K	P/MPa	ρ^b/kg·m^{-3}	$y(\cdot 10^6)$	S/kg·m^{-3} $(\cdot 10^2)$
308.15	15.11	819.12	1.25	9.07
	20.03	863.87	1.27	9.82
	25.06	901.03	1.26	10.14
	30.10	929.59	1.40	11.64
	35.03	949.13	1.92	16.32
318.15	15.05	749.06	1.37	9.06
	20.09	809.66	1.36	9.85
	25.17	857.75	1.42	10.88
	30.06	890.82	1.51	12.03
	35.07	911.57	1.83	14.94
328.15	15.16	662.39	1.43	8.37
	20.09	755.97	1.27	8.57
	25.13	814.53	1.51	11.19
	29.99	851.65	2.19	16.65
	34.83	885.73	2.81	22.04

[a] Standard uncertainties u: $u(T)$ = 0.1 K; $u(P)$ = 0.1 MPa; $u(y)$ = $0.087 \cdot 10^{-6}$; $u(S)$ = $0.63 \cdot 10^{-2}$. [b] Data from NIST webbook (http://webbook.nist.gov/chemistry).

dx.doi.org/10.1021/je301065f | J. Chem. Eng. Data 2012, 57, 3756−3760

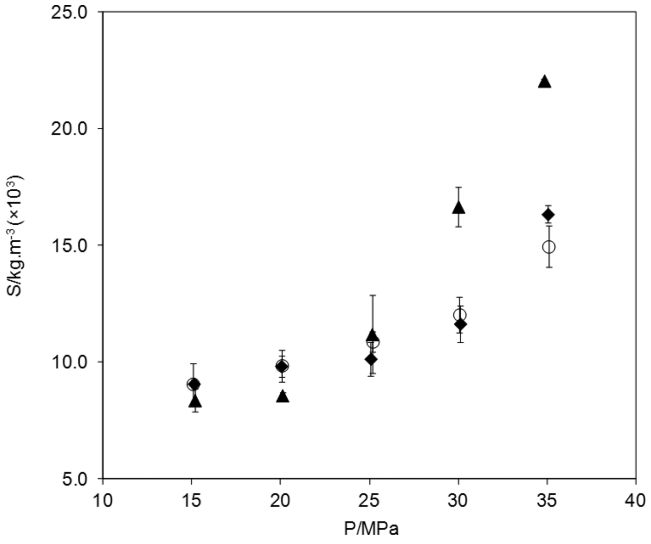

Figure 1. Experimental solubility data of DXMT in $scCO_2$ ($kg \cdot m^{-3}$ of $scCO_2$) at ♦, 308.2 K; ○, 318.2 K, and ▲, 328.2 K.

3, together with the relative standard deviations (RSD) for pressure, for the solid compound mole fractions and for the mass of solid compounds per unit of volume of $scCO_2$. Each reported experimental data point is the average of, at least, three replicate measurements that lead to RSD values lower than 5.8 %. As can be observed, the solubility of DXMT in $scCO_2$ is low, varying between $1.25 \cdot 10^{-6}$ and $2.81 \cdot 10^{-6}$ in terms of mole fraction solubility and between ($9.1 \cdot 10^{-3}$ and $22.0 \cdot 10^{-3}$) $kg \cdot m^{-3}$ in terms of mass of DXMT per unit of volume of $scCO_2$. The minimum and maximum solubility data were measured at 308.2 K at 15.1 MPa and 328.2 K at 34.8 MPa, respectively. The effect of pressure and temperature on the solubility of DXMT is also represented in Figure 1. As expected, and for each isotherm, an increase in pressure leads to an increase in the drug solubility which is more pronounced at higher temperatures (328.2 K), for which an increase of ~96 % is observed between (15 and 35) MPa. This behavior is justified by the enhanced solute−solvent specific interactions that occur when the solvent density increases and that reduces the intermolecular mean distance of the involved molecules. The solubility also increased with temperature, although the density of $scCO_2$ decreases with temperature, however, and considering the experimental error, this effect was only observed between (318.15 and 328.15) K. Moreover, this increase in the solubility of DXMT is more significant at pressures higher than 25 MPa. For example, increasing the temperature from (308.15 to 328.15) K increases the solubility of DXMT by 15 % at 15 MPa, by 19 % at 25 MPa, and by 46 % at 35 MPa. The solubility of solids in $scCO_2$ depends on two mains factors that vary in opposite ways with temperature and which are: (i) the density of the solvent, and consequently its solvency power (which decreases with temperature), and (ii) the volatility of the solute (which increases with temperature). The first effect limits the solubility of the solid drug in the solvent, while the second improves it. This opposite trends usually led to the crossover phenomenon. However and relatively far from the critical point of the solvent, where density has a weaker dependence with temperature, the volatility effect becomes more pronounced than the density effect. In this work, the volatility effect seems to be dominant, and therefore higher solubilities where obtained at higher temperatures. According to Figure 1, the crossover pressure is expected to occur around 15 MPa.

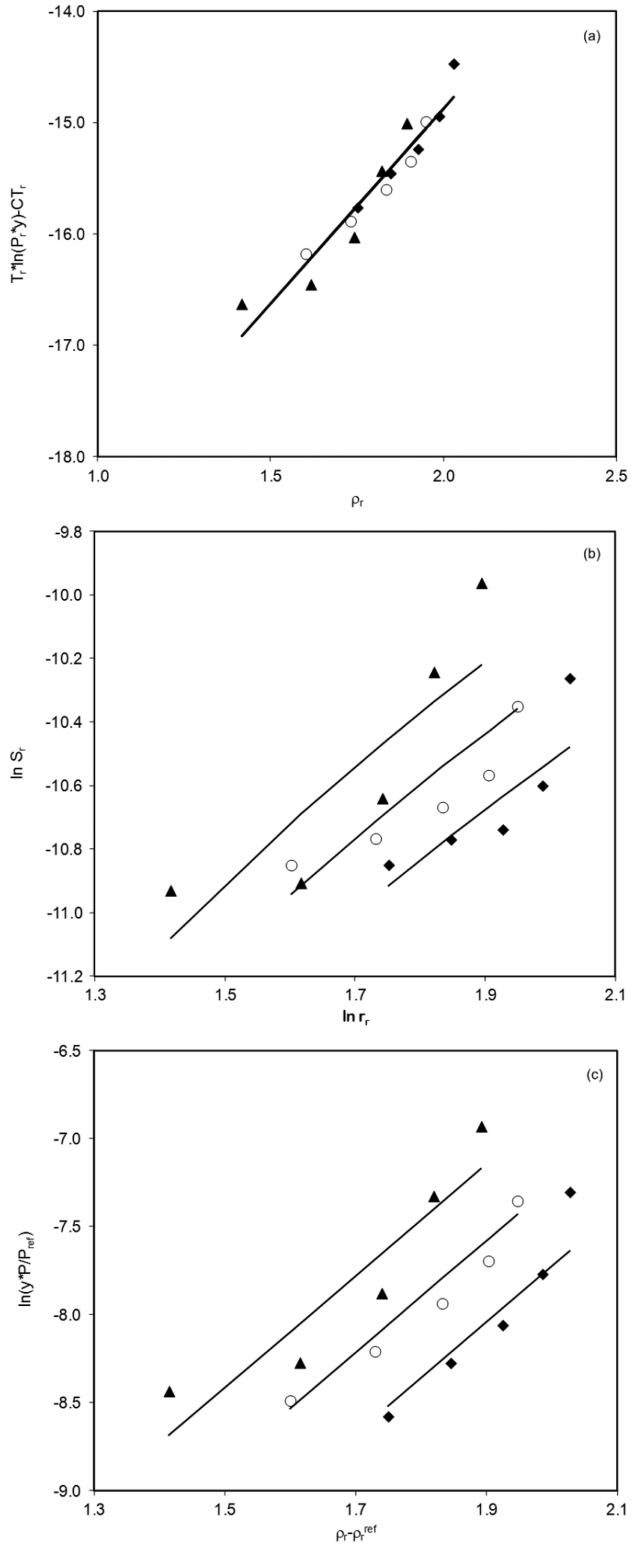

Figure 2. Relationship between the solubility of DXMT and the density of pure CO_2 correlated by the Méndez-Santiago−Teja model (a), by the Chrastil model (b), and by the Bartle model (c) for the isotherms at ♦, 308.2 K; ○, 318.2 K, and ▲, 328.2 K. Lines represent the results obtained from each of the studied models.

To our knowledge experimental data for the solubility of DXMT in $scCO_2$ is presented for the first time in this work.

dx.doi.org/10.1021/je301065f | J. Chem. Eng. Data 2012, 57, 3756−3760

There is a previous work in the literature that presented the solubility of other glucocorticoids (beclomethasone dipropionate, fluticasone proprionate, budesonide) in $scCO_2$, however for a higher temperature [between (338 and 358) K] and pressure [(21.3 and 38.5) MPa] ranges and using a methodology similar to the one used in this work.[39] Authors justified the necessity to use that higher pressure and temperature conditions due to the low solubility of the compounds that varied between $5.93 \cdot 10^{-6}$ (at 338 K and 21.3 MPa) and $3.36 \cdot 10^{-5}$ (at 358 K and 38.5 MPa). In the present work, some modifications were introduced in the experimental methodology as well as in the drug quantification method, as previously described, in order to accurately measure the solubility of DXMT at mild experimental conditions.

The correlation of the measured experimental solubility data was performed using three density-based correlations (Méndez-Santiago–Teja, Bartle, and Chrastil) in terms of reduced variables using the equations presented in Table 2. The correlation results and the corresponding AARD values obtained with the three density-based models are also shown in Table 2 and represented in Figure 2. In general terms the employed models correlate the experimental DXMT solubility in $scCO_2$ with AARD correlation results lower than 13.5 %. However, and as can be seen in Figure 2, none of the models were able to correctly describe the sharp increase in solubility that is verified for each isotherm when pressure increases. As in a previous work,[40] authors tested temperature-dependent models (as the Spark's model[41]), but the improvement was not significant, and the number of adjustable parameters required by this model is excessive considering the number of experimental data points measured. Therefore authors consider that the presented models (specially the Bartle's model) can describe the solubility data dependence on temperature and pressure with acceptable accuracy using a reduced number of adjustable parameters.

CONCLUSIONS

The solid solubility of DXMT in $scCO_2$ was experimentally measured using a static analytical method at (308.2, 318.2, and 328.2) K and for pressures between (15.1 and 35.7) MPa. Data were measured with RSD values lower than 5.8 %. Experimental solubility data were correlated with three density-based models (Chrastil, Bartle, and Méndez-Santiago–Teja models) that led to AARD values lower than 13.5 %, the best results obtained with the Chrastil model. The models were able to correctly describe the temperature dependence but failed to describe the sharp solubility increase that is verified for higher pressures. Nevertheless, the results obtained with the Méndez-Santiago–Teja model confirm the accuracy of the data, and the overall AARD values obtained are acceptable considering the low solubility range measured in this work.

AUTHOR INFORMATION

Corresponding Author

*Tel.: +351 239 798749; fax: +351 239 798703. E-mail addresses: hsousa@eq.uc.pt (H.C.d.S.); adias@eq.uc.pt (A.M.A.D.).

Funding

A.M.A. Dias acknowledges FCT-MCTES for fellowship SFRH/BPD/40409/2007.

Notes

The authors declare no competing financial interest.

REFERENCES

(1) Schacke, H.; Docke, W.; Asadullah, K. Mechanisms involved in the side effects of glucocorticoids. *Pharmacol. Therapeut.* **2002**, *96*, 23–43.

(2) Barnes, P. J. Corticosteroids: The drugs to beat. *Eur. J. Pharmacol.* **2006**, *533*, 2–14.

(3) Ray, J. A.; Kushnir, M. M.; Rockwood, A. L.; Meikle, A. W. Analysis of cortisol, cortisone and dexamethasone in human serum using liquid chromatography tandem mass spectrometry and assessment of cortisol: Cortisone ratios in patients with impaired kidney function. *Clin. Chim. Acta* **2011**, *412*, 1221–1228.

(4) Gallego, J. M. L.; Arroyo, J. P. Simultaneous determination of dexamethasone and trimethoprim by liquid chromatography. *J. Pharm. Biomed. Anal.* **2002**, *30*, 1255–1261.

(5) Bhardwaj, U.; Burgess, D. J. Physicochemical properties of extruded and non-extruded liposomes containing the hydrophobic drug dexamethason. *Int. J. Pharmaceutics* **2010**, *388*, 181–189.

(6) Wadhwa, R.; Lagenaur, C. F.; Cui, X. T. Electrochemically controlled release of dexamethasone from conducting polymer polypyrrole coated electrode. *J. Controlled Release* **2006**, *110*, 531–541.

(7) Kaji, H.; Sugimoto, T.; Kanatani, M.; Nishiyama, K.; Chihara, K. Dexamethasone Stimulates Osteoclast-like Cell Formation by Directly Acting on Hemopoietic Blast Cells and Enhances Osteoclast-like Cell Formation Stimulated by Parathyroid Hormone and Prostaglandin E_2. *J. Bone Miner. Res.* **1997**, *12*, 734–741.

(8) Kim, C. H.; Cheng, S. L.; Kim, G. S. Effects of dexamethasone on proliferation, activity, and cytokine secretion of normal human bone marrow stromal cells: possible mechanisms of glucocorticoid-induced bone loss. *J. Endocrinol.* **1999**, *162*, 371–379.

(9) Nuttlman, C. R.; Tripodi, M. C.; Anseth, K. S. Dexamethasone-functionalized gels induce osteogenic differentiation of encapsulated hMSCs. *J. Biomed. Mater. Res., Part A* **2006**, *76*, 183–195.

(10) Yang, Y.; Tang, G.; Zhang, H.; Zhao, Y.; Yuan, X.; Wang, M.; Yuan, X. Controllable dual-release of dexamethasone and bovine serum albumin from PLGA/β-tricalcium phosphate composite scaffolds. *J. Biomed. Mater. Res., Part B* **2011**, *96B*, 139–151.

(11) Murua, A.; Herran, E.; Orive, G.; Igartua, M.; Blanco, F. J.; Pedraz, J. L.; Hernandez, R. M. Design of a composite drug delivery system to prolong functionality of cell-based scaffolds. *Int. J. Pharmaceutics* **2011**, *407*, 142–150.

(12) Pérez, R. A.; Won, J.; Knowles, J. C.; Kim, H. Naturally and synthetic smart composite biomaterials for tissue regeneration. *Adv. Drug Delivery Rev.* **2012**, DOI: 10.1016/j.addr.2012.03.009.

(13) Su, Y.; Su, Q.; Liu, W.; Lim, M.; Venugopal, J. R.; Mo, X. S. Controlled release of bone morphogenetic protein 2 and dexamethasone loaded in core–shell PLLACL–collagen fibers for use in bone tissue engineering. *Acta Biomater.* **2012**, *8*, 763–771.

(14) Rodrigues, L. B.; Leite, H. F.; Yoshida, M. I.; Saliba, J. B.; Cunha, A. S., Jr.; Faraco, A. A. G. In vitro release and characterization of chitosan films as dexamethasone carrier. *Int. J. Pharmaceutics* **2009**, *368*, 1–6.

(15) Butoescu, N.; Jordan, O.; Burdet, P.; Stadelman, P.; Petri-Fink, A.; Hofmann, H.; Doelker, E. Dexamethasone-containing biodegradable superparamagnetic microparticles for intra-articular administration: Physicochemical and magnetic properties, *in vitro* and *in vivo* drug release. *Eur. J. Pharm. Biopharm.* **2009**, *72*, 529–538.

(16) Kikic, I.; Vecchione, F. Supercritical impregnation of polymers. *Curr. Opin. Solid State Mater. Sci.* **2003**, *7*, 399–405.

(17) Yeo, S.; Kiran, E. Formation of polymer particles with supercritical fluids: A review. *J. Supercrit. Fluids* **2005**, *34*, 287–308.

(18) De Matos, M. B. C.; Piedade, A. P.; C. Alvarez-Lorenzo, Concheiro, A.; Braga, M. E. M.; de Sousa, H. C. SCF-assisted fabrication of dexamethasone-loaded poly(E-caprolactone)/MCM-41 composite materials. Proceedings of the 10th ISSF, International Symposium on Supercritical Fluids, San Francisco, CA, USA, May 13–16, 2012.

(19) Filipe, L. T. R.; Piedade, A. P.; Watkins, J. J.; Braga, M. E. M.; de Sousa, H. C., Bioactive glasses loaded with dexamethasone by a supercritical carbon dioxide deposition process. Proceedings of the

10th ISSF, International Symposium on Supercritical Fluids, San Francisco, CA, USA, May 13−16, 2012.
(20) Thote, A. J.; Gupta, R. B. Formation of nanoparticles of a hydrophilic drug using supercritical carbon dioxide and microencapsulation for sustained release. *Nanomed.: Nanotechnol., Biol., Med.* **2005**, *1*, 85−90.
(21) Duarte, A. R. C.; Mano, J. F.; Reis, R. L. Dexamethasone-loaded scaffolds prepared by supercritical-assisted phase inversion. *Acta Biomater.* **2009**, *5*, 2054−2062.
(22) Duarte, A. R. C.; Mano, J. F.; Reis, R. L. Preparation of chitosan scaffolds loaded with dexamethasone for tissue engineering applications using supercritical fluid technology. *Eur. Polym. J.* **2009**, *45*, 141−148.
(23) Muzzarelli, R. A. A. Chitosan composites with inorganics, morphogenetic proteins and stem cells, for bone regeneration. *Carbohyd. Polym.* **2011**, *83*, 1433−1445.
(24) Reverchon, E.; Della Porta, G. Micronization of antibiotics by supercritical assisted atomization. *J. Supercrit. Fluids* **2003**, *26*, 243−252.
(25) Martin, A.; Cocero, M. J. Micronization processes with supercritical fluids: Fundamentals and mechanisms. *Adv. Drug Delivery Rev.* **2008**, *60*, 339−350.
(26) Pasquali, I.; Bettini, R.; Giordano, F. Solid-state chemistry and particle engineering with supercritical fluids in pharmaceutics. *Eur. J. Pharm. Sci.* **2006**, *27*, 299−310.
(27) Steckel, H.; Thies, J.; Muller, B. W. Micronizing of steroids for pulmonary delivery by supercritical carbon dioxide. *Int. J. Pharmaceutics* **1997**, *152*, 99−110.
(28) Rath, S. N.; Strobel, L. A.; Arkudas, A.; Beier, J. P.; Maier, A. K.; Greil, P.; Horch, R. E.; Kneser, U. Osteoinduction and survival of osteoblasts and bone-marrow stromal cells in 3D biphasic calcium phosphate scaffolds under static and dynamic culture conditions. *J. Cell. Mol. Med.* **2012**, *16*, 2350−2361.
(29) Lucien, F. P.; Foster, N. R. Solubilities of solid mixtures in supercritical carbon dioxide: a review. *J. Supercrit. Fluids* **2000**, *17*, 111−134.
(30) Coimbra, P.; Fernandes, D.; Ferreira, P.; Gil, M. H.; de Sousa, H. C. Solubility of Irgacure 2959 photoinitiator in supercritical carbon dioxide: Experimental determination and correlation. *J. Supercrit. Fluids* **2008**, *45*, 272−281.
(31) Duarte, A. R. C.; Santiago, S.; de Sousa, H. C.; Duarte, C. M. M. Solubility of Acetazolamide in Supercritical Carbon Dioxide in the Presence of Ethanol as a Cosolvent. *J. Chem. Eng. Data* **2005**, *50*, 216−220.
(32) Coimbra, P.; Fernandes, D.; Gil, M. H.; de Sousa, H. C. Solubility of Diflunisal in Supercritical Carbon Dioxide. *J. Chem. Eng. Data* **2008**, *53*, 1990−1995.
(33) Coimbra, P.; Gil, M. H.; Duarte, C. M. M.; Heron, B. M.; de Sousa, H. C. Solubility of a spiroindolinonaphthoxazine photochromic dye in supercritical carbon dioxide: Experimental determination and correlation. *Fluid Phase Equilib.* **2005**, *238*, 120−128.
(34) Coimbra, P.; Blanco, M. R.; Silva, H. S. R. C.; Gil, M. H.; de Sousa, H. C. Experimental Determination and Correlation of Artemisinin's Solubility in Supercritical Carbon Dioxide. *J. Chem. Eng. Data* **2006**, *51*, 1097−1104.
(35) Calza, P.; Pelizzetti, E.; Brussino, M.; Baiocchi, C. Ion trap tandem mass spectrometry study of dexamethasone transformation products on light activated TiO_2 surface. *J. Am. Soc. Mass Spectrom.* **2001**, *12*, 1286−1295.
(36) Mendez-Santiago, J.; Teja, A. S. The solubility of solids in supercritical fluids. *Fluid Phase Equilib.* **1999**, *158−160*, 501−510.
(37) Bartle, K. D.; Clifford, A. A.; Jafar, S. A. Solubilities of Solids and Liquids of Low Volatility in Supercritical Carbon Dioxide. *J. Phys. Chem. Ref. Data* **1991**, *20*, 713−757.
(38) Chrastil, J. Solubility of solids and liquids in supercritical gases. *J. Phys. Chem.* **1982**, *86*, 3016−3021.
(39) Vatanara, A.; Najafabadi, A. R.; Khajeh, M.; Yamini, Y. Solubility of some inhaled glucocorticoids in supercritical carbon dioxide. *J. Supercrit. Fluids* **2005**, *33*, 21−25.
(40) Chim, R.; Marceneiro, S.; Braga, M. E. M.; Dias, A. M. A.; de Sousa, H. C. Solubility of norfloxacin and ofloxacin in supercritical carbon dioxide. *Fluid Phase Equilib.* **2012**, *331*, 6−11.
(41) Sparks, D. L.; Hernandez, R.; Estévez, L. A. Evaluation of density-based models for the solubility of solids in supercritical carbon dioxide and formulation of a new model. *Chem. Eng. Sci.* **2008**, *63*, 4292−4301.